CLM-P 397

ELECTRON CYCLOTRON EMISSION FROM A TOKAMAK PLASMA

EXPERIMENT AND THEORY

A.E. Costley*, R.J. Hastie, J.W.M. Paul, J. Chamberlain*

(Submitted for publication in Phys. Rev. Lett.)

A B S T R A C T

We present the first measurements of the power, polarization and frequency spectrum of the electron cyclotron emission from a tokamak plasma. The radiation is not polarized, does not have the previously predicted spectrum, and under certain circumstances is an order of magnitude above the predicted power level. We interpret the results in terms of a scrambling of polarization on reflection within the torus and in terms of the emission from supra-thermal electrons.

* National Physical Laboratory, Teddington, Middlesex.

UKAEA Research Group,

Culham Laboratory,

Abingdon,

Oxfordshire

July 1974

Electron cyclotron emission from hot toroidal plasmas is currently of importance in fusion research. It is anticipated that it could constitute a significant power loss in a reactor[1,2] and that a measurement of it could be an informative plasma diagnostic technique[3].

In this letter we present measurements of the electron cyclotron emission (occurring at millimetre wavelengths) from the hot plasma of a tokamak device. To explain our results we include in the theory of this emission, polarization scrambling on reflection within the torus, and some of the possible effects of a relatively small run-away electron component.

The plasma investigated is produced by the CLEO-TOKAMAK[4]. It has a toroidal flux density $B_\varphi \leq 2.0$ T, a mean electron density $n_e \sim 2 \times 10^{19}$ m^{-3}, a central electron temperature $T_{eo} \sim 300$ eV, a central ion temperature $T_{io} \sim 200$ eV, a major radius $R_o = 0.9$ m, a minor radius $a_o = 0.18$ m and duration up to 180 ms.

EMISSION MEASUREMENTS: These were made by observing the plasma along a major radius through a wedge shaped window of crystal quartz (z-cut). A Fourier transform measurement technique was used. Radiation from the plasma was directed into a two-beam polarization-type interferometer[5]. The path-difference (x) within this, was scanned in 10 ms over the range $-1 \text{ mm} < x < 9 \text{ mm}$ by oscillation of one of the interferometer mirrors, and the resulting interference patterns (Fig. 1) were detected with a Putley indium antimonide detector. (The spectrally integrated emission was also detected for reference purposes). Subsequent Fourier transformation of the interference patterns and calibration of the apparatus yielded the emission spectra.

In the calibration the time-dependence of the path-difference was

measured using an HCN laser (λ = 337 μm) and the absolute power response of the interferometer/detector arrangement was determined with a dc mercury arc lamp. Such lamps have been shown previously[6] to radiate approximately as a black-body with a radiation temperature of 3000 K.

The emission spectrum from a typical tokamak shot is shown in Fig. 2 (curve a). The resolution in the spectrum is determined by the total scan x_m used in the Fourier transform, $R = cx_m^{-1}$, and in this case is 37.5 GHz. As expected emission peaks occur at the cyclotron harmonics ($n\omega_{ce}$) n = 2, 3 and 4 for the magnetic field B_o at the centre of the plasma. The emission at n = 1 (ie I_1) could not be deduced by the normal procedure since the calibration system was insensitive in this region. However, from the known responsivity of the Putley detector an upper limit can be placed on I_1 as in Fig. 2.

By combining data recorded on two identical tokamak shots spectra with an improved resolution of 25 GHz were obtained (Fig. 2 b). A mirror in the fixed arm of the interferometer was displaced between the two shots so that adjacent parts of the interference patterns were scanned, and composite interference patterns were constructed and transformed.

Variation of the tokamak conditions revealed a clear correlation between the level and spectrum of the emission (eg Fig 2 c), and the level of hard X-ray emission. (Note that the latter is an indication of the presence of high energy runaway electrons). Under conditions of relatively intense X-ray emission the spectrally unresolved monitor showed an increase of up to an order of magnitude in emitted power.

The uncertainties in the measurement method are such that the

relative shape and frequency position of the spectral features are reliable to about ± 10%, and that the absolute level of the spectra is reliable to about an order of magnitude (ie factor of 3 either way). The latter uncertainty arises mainly from the need to use different optical and electronic systems for the calibration and the plasma measurements. The emission in the region of $4\omega_{ce}$ is subject to a ± 20% uncertainty because of the presence of a small unidentified feature at about 225 GHz in the calibration data. The effect of smoothing this feature is shown in Fig. 3.

POLARIZATION MEASUREMENTS: The orientation of a wire polarizer in the interferometer was changed between discharges and the resulting interference patterns were recorded. Since the transformed spectra were the same to within the discharge reproducibility limits (± 10%), the detected radiation was unpolarized (to within this uncertainty) at all frequencies in the region examined.

In a separate experiment an optical system of smaller étendue, which excluded radiation reflected in the torus side-arm, was used, and spectrally integrated signals were recorded. Since these were independent of the orientation of a wire polarizer mounted in the optical system, we conclude that the radiation that crossed the plasma/vacuum boundary was unpolarized.

In an effort to understand this lack of polarization we measured the depolarizing effect of multiple reflections within the stainless steel torus. With no plasma present the torus was irradiated with a polarized beam of 2 mm wavelength radiation and the polarization state of the radiation emanating from several radial ports was determined. While radiation from a port immediately adjacent to the entrance port ($\varphi = 20^{\circ}$) was partially polarized that from other ports with $\varphi \geq 90^{\circ}$

was less than $\pm$ 10% polarized demonstrating that multiple reflections within the torus can depolarize the radiation.

THEORY FOR POLARIZED EMISSION: The radiation transport equation for the intensity[7] $I_g(\omega)$ in each mode (extraordinary g = e, ordinary g = o) within a slab of magnetized plasma with specific emission $\eta_g(\omega)$ and absorption $\alpha_g(\omega)$, along a path s perpendicular to the field is

$$\frac{dI_g(\omega,s)}{ds} = \eta_g(\omega,s) - \alpha_g(\omega,s) I_g(\omega,s). \qquad (1)$$

Combining this with Kirchhoff's Law $\eta_g = \alpha_g I_B$, where the single mode black-body emission $I_B = \omega^2 kT_e/8\pi^3 c^2$, and allowing for the presence of a metal wall, with reflection coefficient $r = r(\omega)$ bounding the plasma, yields the solution[8]

$$I_g = I_B [1 - \exp(-\int \alpha_g ds)]/[1 - r \exp(-\int \alpha_g ds)]. \qquad (2)$$

At frequencies for which the slab is optically thin, (i.e. $\int \alpha_g ds << 1 - r$),

$$I_g = I_B \int \alpha_g ds/(1 - r) \qquad (3)$$

and optically thick, (i.e. $\int \alpha_g ds >> 1 - r$), $I_g = I_B$. (4)

We now consider the theoretical cyclotron emission from a toroidal plasma in the direction of the major radius[2,3] (non-relativistic limit for $T_e \sim 300$ eV). The spatial contributions are integrated across the toroidal profile with arbitrary $n_e(s)$, $T_e(s)$ and defined $B(s) = B_o(1 - s/R_o)$. For each ω and harmonic n the resonance $\omega = n\omega_{ce}(s_r) = n\omega_{ce}(o)\,(1 + s_r/R_o)$ defines the position s_r. The total emission is then given by equation (2) with

$$\int \alpha_e ds = \sum_{n=1}^{\infty} n_e(s_r) \left[\frac{kT_e(s_r)}{2mc^2}\right]^{n-1} \frac{n^{2n-2}}{(n-1)!} \left(\frac{\pi e R_o}{\varepsilon_o B_o c}\right). \qquad (5)$$

The electron temperature can be determined from the ratio of any two

harmonics provided they are not both optically thick.

The values of $\int \alpha_e ds$ for CLEO-TOKAMAK are listed in Table I together with $1 - r(\omega)$ for stainless steel. We note that harmonics $n < 3$ are optically thick, $n > 3$ are optically thin, while $n = 3$ is intermediate.

TABLE I

	n = 2	n = 3	n = 4
$\int \alpha_e ds$	1.00	2.96×10^{-3}	1.46×10^{-5}
$1 - r(\omega)$	5.46×10^{-3}	6.69×10^{-3}	7.72×10^{-3}

For our conditions the spectral widths of the various harmonics are determined by the toroidal inhomogeneity of the field. This inhomogeneity gives overlap of harmonics n = 3 and 4. However provided the profiles of $n_e(s)$ and $T_e(s)$ are not particularly flat, the main emission peaks can be calculated separately.

In Fig. 2 we have plotted the predictions of this model for the parameters of the CLEO-TOKAMAK with the measured parabolic $n_e(s)$, assuming a parabolic $T_e(s)$. We find that

(i) the measured absolute magnitudes exceed the predictions by more than the estimated factor of three uncertainty. To fit I_2 (Fig. 2) to a black-body curve would require $T_e = 1.9$ keV.

(ii) the measured ratios of the intensities of the harmonics yield predicted electron temperatures: $I_3/I_2 \Rightarrow 280$ eV, $I_4/I_2 \Rightarrow 1.1$ keV.

However the main discrepancy is the observed absence of polarization.

THEORY FOR UNPOLARIZED EMISSION: We now assume, on the basis of the subsidiary experiment mentioned above, that each reflection produces some scrambling of the polarizations. We define a transfer fraction p between the two polarizations at each reflection. The boundary condition for the reflected intensity, I', then becomes

$$I'_{(o,e)} = r\{I_{(o,e)} + p\,[I_{(e,o)} - I_{(o,e)}]\} \tag{6}$$

and the transport equation with $\alpha_o = 0$ yields a solution

$$I_e = I_B\,[1 - \exp(-\int\alpha_e ds)]/[1 - \hat{r}\,\exp(-\int\alpha_e ds)]$$

$$I_o = I_e\,rp/(1 - r + rp) \tag{7}$$

where $\hat{r} = r\,[1 - p\,(1 - r)/(1 - r + rp)]$.

From these equations we see that the emission is completely unpolarized, ie $I_e = I_o$ for all n, when

$$1 - r << rp \approx p. \tag{8}$$

In this limit we also find that

$$1 - \hat{r} = 2\,(1 - r). \tag{9}$$

We now consider the two cases of unpolarized emission

(i) Optically thin, i.e. $\int\alpha_e ds << 1 - \hat{r} = 2\,(1 - r)$ for which

$$I_o = I_e = I_B\int\alpha_e ds/(1 - \hat{r}) = \tfrac{1}{2}I_B\int\alpha_e ds/(1 - r). \tag{10}$$

The total intensity $(I_o + I_e)$ is the same as for $p = 0$.

(ii) Optically thick, i.e. $\int\alpha_e ds >> 1 - \hat{r}$ for which

$$I_o = I_e = I_B. \tag{11}$$

Each mode is limited by the same black-body curve as for p = 0 and so the two modes give twice the total intensity.

The predictions of this theory for our parameters assuming inequality (8) are plotted in Fig. 3. The observed absolute magnitude of I_2 exceeds the prediction by a factor 3.4, just outside the estimated uncertainty. The observed ratios of the peaks yield predicted electron temperatures $I_3/I_2 \Rightarrow 400$ eV, $I_4/I_2 \Rightarrow 1.4$ keV. Even allowing for the calibration uncertainty, the discrepancy in I_4 is large and we must look for an alternative explanation for this emission, in particular in terms of runaway phenomena.

EMISSION WITH RUNAWAY ELECTRONS: In the presence of a longitudinal electric field the electron distribution function contains a high energy runaway region and a region of isotropic enhancement of the Maxwellian tail at lower energies. For simplicity we simulate these distortions by a second Maxwellian distribution with temperature $T_2 >> T_1$ and density $n_2 << n_1$. The above emission formulae are valid for a double Maxwellian velocity distribution provided that, for the n^{th} harmonic[9]

(i) we replace T_e in I_B by $(n_1 T_1^{\,n} + n_2 T_2^{\,n})/(n_1 T_1^{\,n-1} + n_2 T_2^{\,n-1})$ (12)

(ii) we replace $n_e T_e^{\,n-1}$ in $\int \alpha_e ds$ by $(n_1 T_1^{\,n-1} + n_2 T_2^{\,n-1})$. (13)

In general the second Maxwellian will tend to relatively increase the emission at the higher harmonics, such as is seen for I_4. We can use the measured ratios I_3/I_2 and I_4/I_2 together with $n_1 = n_e$ and $T_1 = T_{eo}$ to determine independent values $T_2 \sim 57$ keV and $n_2 \sim 1.6 \times 10^{12}$ m^{-3}.

One important characteristic of the spectrum observed for high runaway conditions (Fig.2c) is the dominant broad peak at $\omega \sim 3.3\omega_{ce}$. Overlapping of I_3 and I_4 in the region $3.2 < \frac{\omega}{\omega_{ce}} < 3.6$ could occur for

flat profiles $n_e(s)$ and $T_e(s)$. The above values of n_2 and T_2 are consistent with the ratio of this broad peak to I_2.

DISCUSSION: It is possible, in view of the uncertain absolute calibration, to assume that the second harmonic in Fig. 3 fits the predicted curve for unpolarized emission (ie $2I_B(\omega)$) for the measured $T_e \sim 300$ eV. This change of calibration implies that the predicted fundamental emission should be above the limit of detectability, but it is not seen. However, the extraordinary mode fundamental would be reflected in the decreasing B_φ at the upper-hybrid region[10,11]. The remaining ordinary mode would fall below detectability, consistent with observation.

On the other hand, if I_2 really is well above $2I_B$ (Fig. 3) then we have to explain the supra-thermal emission even for n = 2.

The main implications of this work are (i) diagnostic applications may be confused by runaway phenomena, (ii) the power balance of a fusion reactor may be adversely affected by the enhanced cyclotron emission[12] arising from the depolarization and the runaway effects.

We wish to acknowledge discussions with Dr D.D. Burgess, Dr R.J. Bickerton and Mr E. Puplett and assistance from the CLEO-TOKAMAK team and Mr J. Weaver.

REFERENCES:

[1] B.A. Trubnikov, A.E. Bazhanova, Plasma Physics and the Problem of Controlled Thermonuclear Reactors (Ed. M.A. Leontovich) 3, 141 (1959).

[2] M.N. Rosenbluth, Nucl. Fusion 10, 340 (1970).

[3] F. Engelmann and M. Curatolo, Nucl. Fusion 13, 497 (1973).

[4] J.W.M. Paul et al. Sixth European Conference on Controlled Fusion and Plasma Physics, Moscow, (1973).

[5] D.H. Martin and E. Puplett, Infra-red Phys. 10, 105 (1970).

[6] A.H. Lichtenberg and S. Sesnic, J. Opt. Soc. Amer. 56, 75 (1966).

[7] Strictly spectral radiance in $Wm^{-2}\ sr^{-1}\ rad^{-1}\ s$.

[8] G. Bekefi, Radiation Processes in a Plasma, Wiley, New York 1966, p 41.

[9] G. Bekefi, J.L. Hirshfield and S.C. Brown. Phys. Fluid 4, 173 (1961).

[10] H. Dreicer. NATO Advanced Study Institute on Plasma Waves in Space and the Laboratory, Roros, Norway (1968).

[11] A.N. Dellis, Private communication.

[12] We should also like to point out that irregular reflections will also enhance the emission in directions not perpendicular to B_φ.

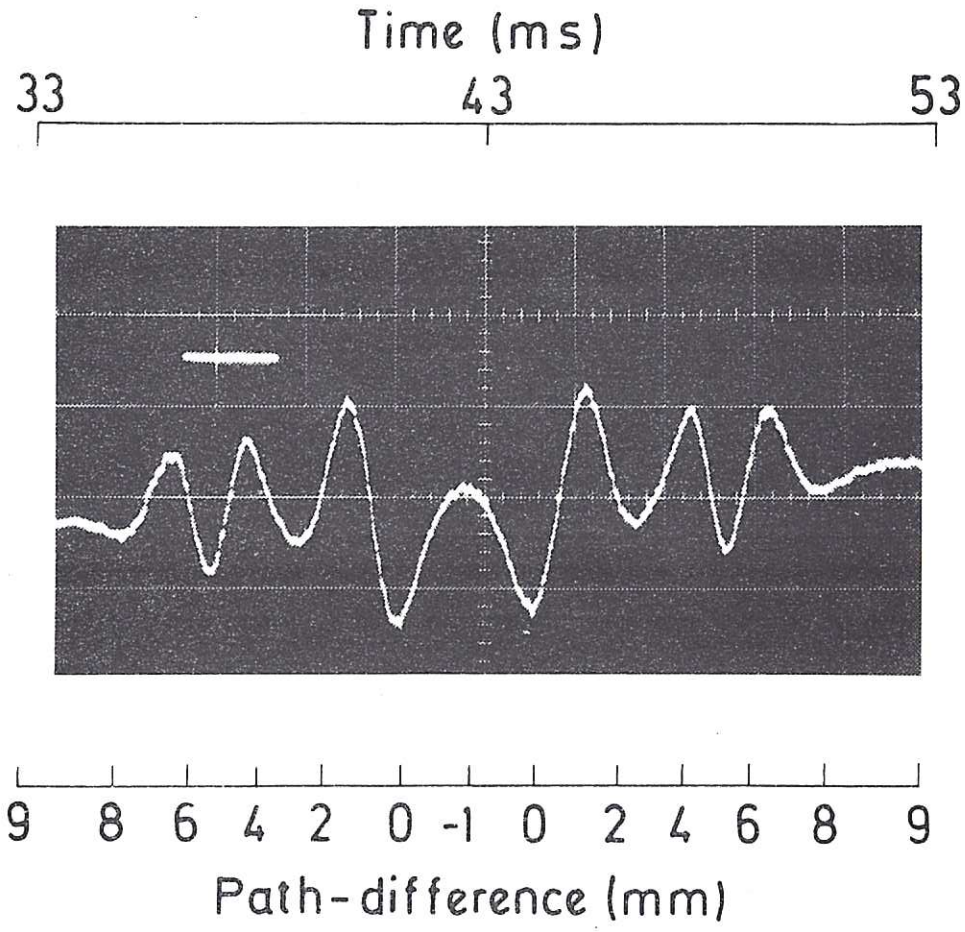

Fig.1. Signal from the interferometer showing two scans of the interference pattern, traversed in opposite directions. (Time is from initiation of discharge).

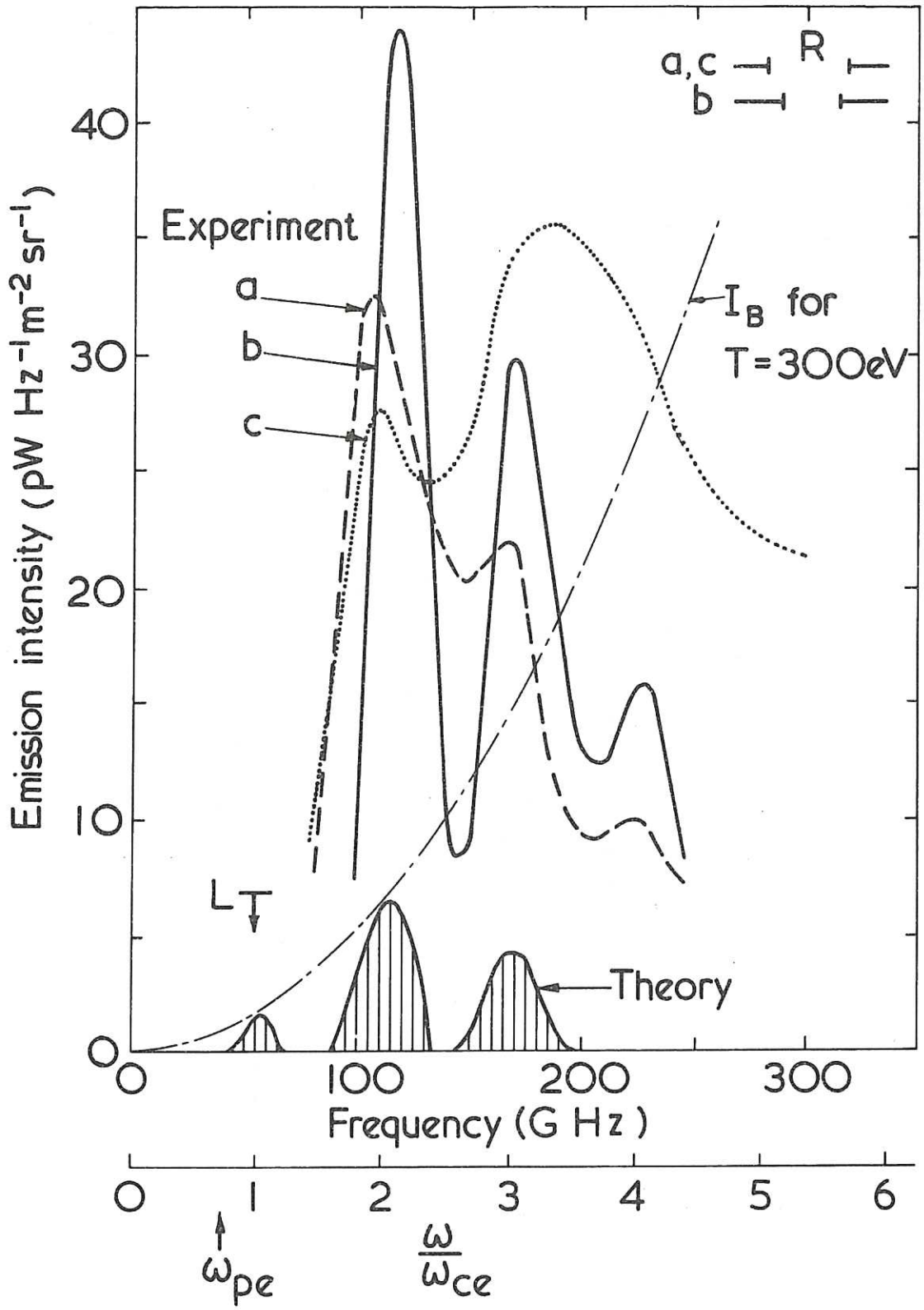

Fig.2. Emission spectra: Experiment (a) single scan from Fig.1, (b) composite scan (c) single scan but with appreciable runaway (L = limit of detectability); theoretical prediction for polarized emission (extraordinary mode vertical hatching, ω_{pe} is plasma frequency).

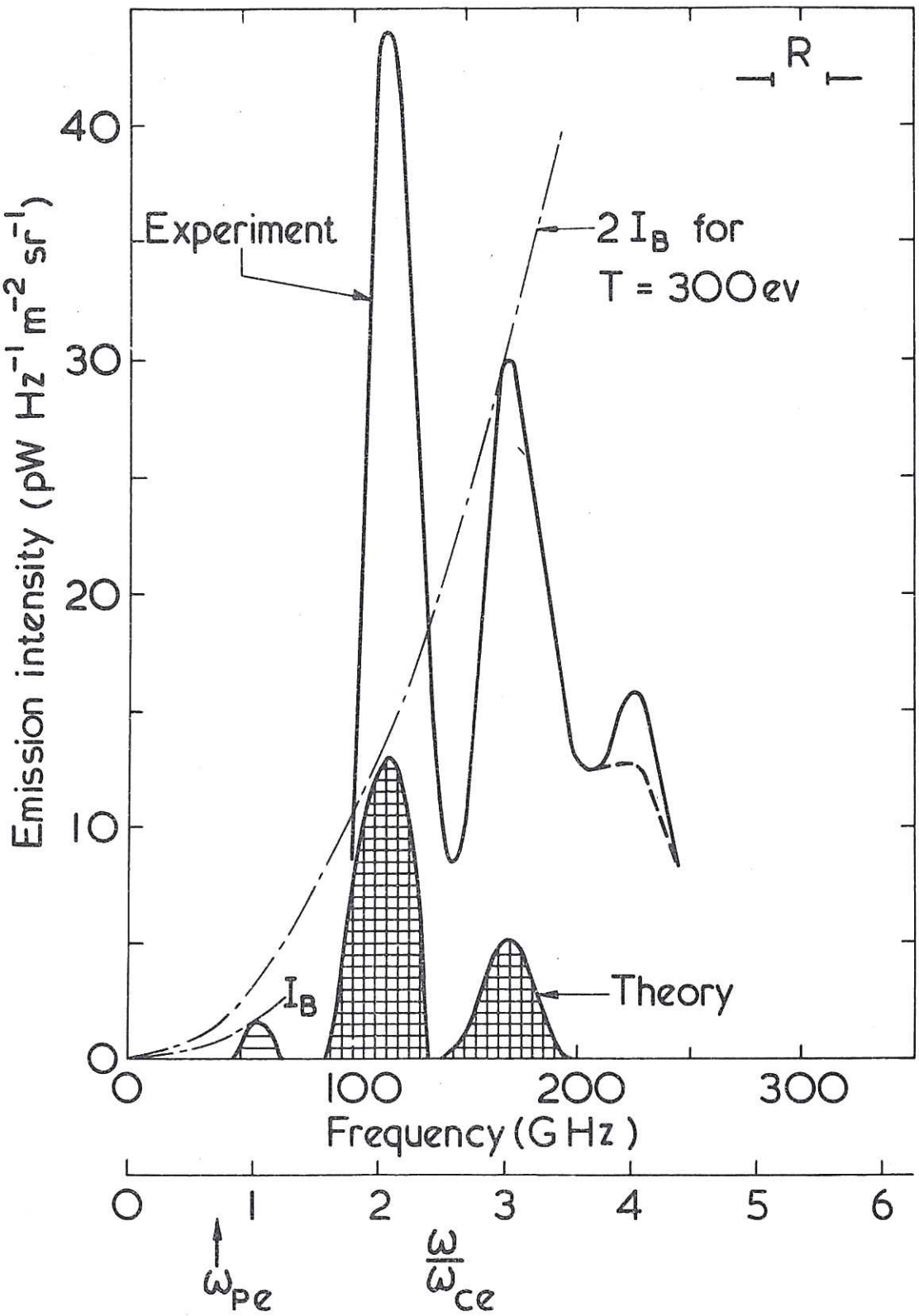

Fig.3. Emission spectra: Experiment, composite scan (effect of smoothed calibration at n = 4, dashed line); theoretical, prediction with polarization scrambling (Ordinary mode horizontal hatching and unpolarized cross hatching).